© 2021. Published by The Company of Biologists Ltd | Development (2021) 148, dev195545. doi:10.1242/dev.195545

RESEARCH REPORT

# Cantil: a previously unreported organ in wild-type *Arabidopsis* regulated by FT, ERECTA and heterotrimeric G proteins

**Timothy E. Gookin* and Sarah M. Assmann***

## ABSTRACT

We describe a previously unreported macroscopic *Arabidopsis* organ, the cantil, named for its 'cantilever' function of holding the pedicel at a distance from the stem. Cantil development is strongest at the first nodes after the vegetative to reproductive inflorescence transition; cantil magnitude and frequency decrease acropetally. Cantils develop in wild-type *Arabidopsis* accessions (e.g. Col-0, Ws and Di-G) as a consequence of delayed flowering in short days; cantil formation is observed in long days when flowering is delayed by null mutation of the floral regulator *FLOWERING LOCUS T*. The receptor-like kinase ERECTA is a global positive regulator of cantil formation; therefore, cantils never form in the *Arabidopsis* strain L*er*. ERECTA functions genetically upstream of heterotrimeric G proteins. Cantil expressivity is repressed by the specific heterotrimeric complex subunits GPA1, AGB1 and AGG3, which also play independent roles: GPA1 suppresses distal spurs at cantil termini, while AGB1 and AGG3 suppress ectopic epidermal rippling. These G protein mutant traits are recapitulated in long-day flowering *gpa1-3 ft-10* plants, demonstrating that cantils, spurs and ectopic rippling occur as a function of delayed phase transition, rather than as a function of photoperiod per se.

**KEY WORDS: *Arabidopsis thaliana*, Phase transition, Heterotrimeric G proteins, ERECTA, Flowering time, Inflorescence morphology**

## INTRODUCTION

Despite the phenotypic variation of individuals, organisms customarily reach a final, generalized body plan that is characteristic of the species. In plants, this plan is plastic, as the indeterminate plant body allows recurrent addition or suppression of distinct organs (e.g. leaves, branches and flowers), thereby fine-tuning the developing plant architecture to the environment. For example, as a facultative long-day plant, short days (SDs) promote *Arabidopsis thaliana* vegetative growth and delay flowering, while long days (LDs) stimulate flowering (Giakountis et al., 2010). The archetypal architecture of *Arabidopsis* plants is well established (Provart et al., 2016) and, at maturity, *Arabidopsis* plants exhibit three distinct metamers: a basal rosette bearing leaves (M1), an upright co-florescence-producing proximal primary stem (M2) and a distal stem segment bearing nodes that directly produce single flowers borne on a pedicel (M3) (Fig. 1A). Archetypal pedicel attachment is exemplified by upward-slanting pedicels that emerge directly from the stem (Fig. 1B) (Denay et al., 2017).

Department of Biology, The Pennsylvania State University, University Park, PA 16802, USA.

*Authors for correspondence (sma3@psu.edu; tegookin@gmail.com)

T.E.G., 0000-0002-0994-0790; S.M.A., 0000-0003-4541-1594

**Handling Editor: Ykä Helariutta**
**Received 28 July 2020; Accepted 26 April 2021**

Pedicel emergence directly from archetypal M3 nodes, without a lateral intermediary structure, is a robust feature that previous publications suggest is controlled by specific genetic determinants; overexpression of multiple proteins, in both *Arabidopsis* and *Brassica napus* (canola), causes atypical development of a supporting structure basal to the pedicel (Kirik et al., 1998; Wen and Walker, 2006; Dumonceaux et al., 2009; Ikeuchi et al., 2011; Colling et al., 2015). These gain-of-function studies point towards the existence of a signaling cascade that restricts pedicel attachment directly to the stem, yet do not conclusively identify any of the components, particularly as overexpression can result in neomorphic effects.

In our work, we noticed the infrequent occurrence of similar M3 node morphological deviations in diverse *Arabidopsis* knockout lines, particularly in null mutants of the heterotrimeric G protein complex. Heterotrimeric G protein complexes, comprising Gα, Gβ and Gγ subunits, function as conserved eukaryotic signaling hubs that play fundamental roles in development and environmental responses (Urano et al., 2016b). Plant Gα and Gβ proteins are known to modulate the size of the shoot apical meristem (SAM) (Bommert et al., 2013; Ishida et al., 2014; Urano et al., 2016a), which is the progenitor of emergent aboveground organs, and localization of the sole canonical *Arabidopsis* Gα (GPA1) and sole Gβ (AGB1) subunits in the SAM is well documented (Weiss et al., 1993; Huang et al., 1994; Anderson and Botella, 2007; Ishida et al., 2014). G protein signaling specificity is achieved via 12 distinct G protein complexes in *Arabidopsis* via the association of GPA1 (Gookin and Assmann, 2014), or of one of three atypical extra-large Gα subunits (XLG1, XLG2 and XLG3) (Chakravorty et al., 2015), with one of three obligate Gβγ dimers (AGB1-AGG1, AGB1-AGG2 or AGB1-AGG3). In each case, dissociation of the complex leads to free Gα and Gβγ dimers, which can signal to additional effectors (Urano et al., 2013). Through observation, we linked the infrequent morphological deviations we observed in LDs to wild-type and mutant *Arabidopsis* plants that were initially grown for an extended time period in SDs. Here, we identify the wild-type expressivity of these M2-M3 transition morphologies, the underlying requirements for their development, and specific positive and negative genetic determinants that govern their formation.

### Cantil formation in wild-type plants

Wild-type *Arabidopsis* accession Columbia (Col-0) plants flowering under SD (8-10 h) morphologically deviate from the archetypal pedicel arrangement by developing a macroscopic anatomical structure we call a 'cantil', for cantilever, as it holds the pedicel at a distance from the stem (Fig. 1C-E). Cantils originate from the stem without an obvious junction but terminate at a distinct junction that holds a single pedicel at an angle (~25-90°). The typical upward arc of longer cantils (Fig. 1E) is less obvious on shorter cantils (Fig. 1D), and, at its weakest, cantil growth is limited

Development (2021) 148, dev195545. doi:10.1242/dev.195545

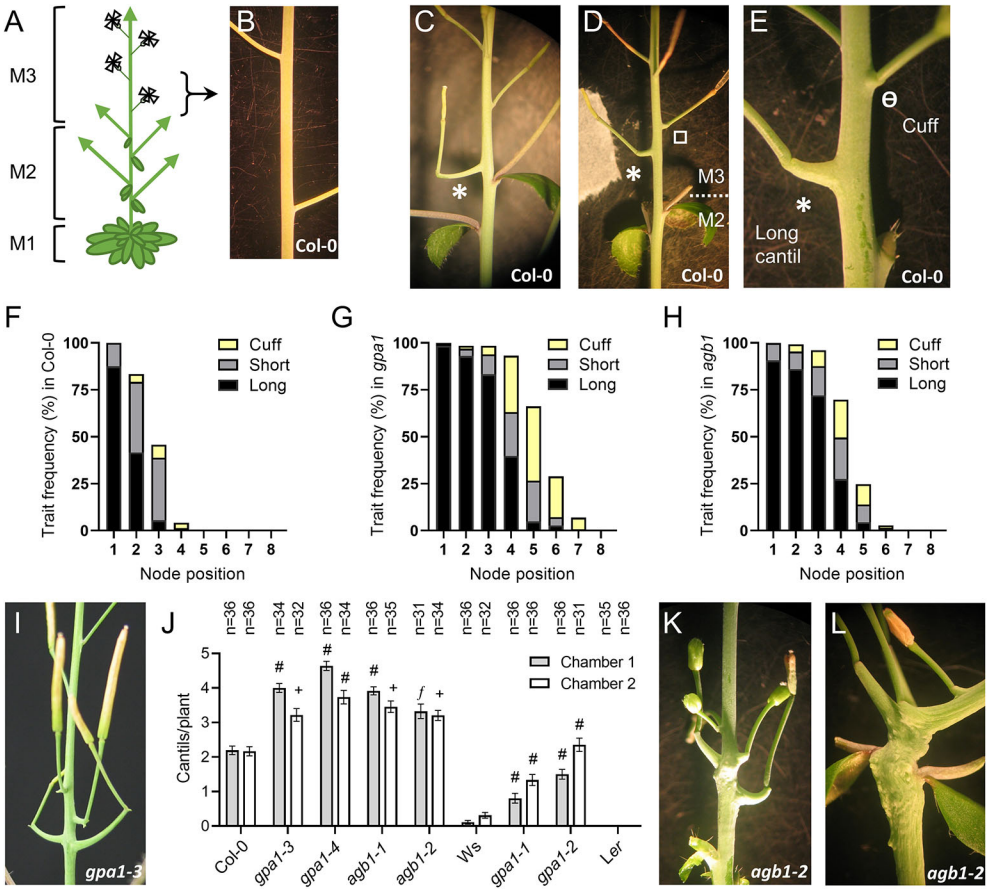


**Fig. 1. Wild-type cantils develop in short days; cantil size and frequency are enhanced by loss of GPA1 or AGB1.** (A) *Arabidopsis* architecture schematic, with the three metamers (M1, M2 and M3) indicated. Bracket indicates the region shown in B. (B) LD Col-0 image showing the archetypal pedicel attached directly to the stem. (C-E) Short-photoperiod architecture for Col-0 with (C) one long cantil (asterisk), (D) one long (asterisk) and a subsequent short cantil (square) (i.e. ∼1 mm long, without tapering characteristic of long cantils), and (E) Col-0 exhibiting one long cantil and a subsequent cuff (θ) (i.e. a swelling that encircles and raises the pedicel base). (F-H) Acropetal positional assessment of cantil development expressed as the percentage of plants exhibiting the trait (cuff, or short or long cantil) at the specified nodal position relative to the M2-M3 junction. Experiments quantified in J. (F) Col-0, (G) *gpa1* (Col) and (H) *agb1* (Col). (I) Representative *gpa1* architecture; *gpa1-3* is shown. (J) Quantitative analysis of SD cantil formation in two large-scale experiments. Data are mean±s.e.m., $n$=619 plants comprising nine genotypes. Statistical significance for differences from the respective wild type are $^{\#}P$<0.0001, $^{+}P$<0.0006 and $^{f}P$=0.0016 (one-way ANOVA with Dunnett's test). (K,L) Representative *agb1* architecture: (K) *agb1-2* displaying cantils; (L) *agb1-2* with extensive rippling and angled stem.

to a 'cuff' that comprises an unelongated cantil that encircles the entire pedicel base (Fig. 1E; see Fig. S1A-E for phenotype overview). In wild-type Col-0 plants, the magnitude and frequency of cantil display is most prominent nearest the M2-M3 junction (Fig. 1D and Fig. S1B-D), and characteristically decreases acropetally with pedicel position (Fig. 1F). SD-grown wild-type Wassilewskija (Ws) plants produce cantils that are morphologically similar to those of Col-0 (Fig. S1F), but do so 10-fold less frequently (Fig. S1G). Notably, the widely used Landsberg *erecta* (L*er*) strain fails to produce any cantils or cuffs (Fig. S1G,H). When flowering in LD (16 h), wild-type Col-0 very rarely deviates from the archetypical form, e.g. producing only two cantils and three cuffs in >3635 inspected pedicels from 727 plants (Fig. S1G,I). No cantils were observed for Ws or L*er* flowering in LD (Fig. S1G). These results suggest the variable penetrance and expressivity of wild-type cantil formation (Col-0>Ws>L*er* and SD>LD) is controlled by distinct genetic elements.

## G proteins repress cantil frequency

Col-0 background *gpa1* (Fig. 1G) and *agb1* (Fig. 1H) mutants flowering in SD produce cantils with increased magnitude and frequency at each M3 inflorescence pedicel position relative to wild-type Col-0 (Fig. 1F, Fig. S1B-E). Null mutation of GPA1 or AGB1 extends the cantil developmental range to distal M3 nodes (Fig. 1G,H), with altered developmental patterning most evident distally adjacent to the M2-M3 junction (e.g. *gpa1-3* in Fig. 1I, Figs S1E and S2A). Total cantil data from our two large-scale experiments showed that *GPA1*-null mutants in both the Col-0 (*gpa1-3* and *gpa1-4*) and Ws (*gpa1-1* and *gpa1-2*) backgrounds develop significantly more cantils in SD than do wild type (Fig. 1J). These differences are not explained by decreased co-florescence production (Fig. S2B) or by failed cuff elongation as all four *gpa1* alleles also developed cuffs at a higher frequency (Fig. S2C). Similarly, SD-flowering *AGB1* null mutants in the Col-0 background (*agb1-1* and *agb1-2*) developed significantly more cantils than wild type (Fig. 1J,K). AGB1 also represses another phenotype, ectopic epidermal rippling (Fig. 1K,L), which formed at the M2-M3 junction in 84% of *agb1* mutants (Fig. S2D). This rippling was often accompanied by very short internodes and a distal stem exiting the junction at an angle (Fig. 1L and Fig. S2E,F). Although primarily diagnostic for *agb1*, minor rippling and angled junctions appeared in 2% of *GPA1* mutants (Fig. S2D). Like wild

Development (2021) 148, dev195545. doi:10.1242/dev.195545

type, no cantils, ectopic rippling or altered stem angles were observed in *gpa1-1*, *gpa1-3* or *agb1-2* grown through flowering in LD (Fig. S2D), indicating these phenotypes are tightly linked to SD conditions. Under SD, cantil/plant averages were increased by 67% in *gpa1* and 52% in *agb1* mutants in the Col-0 background, and by a striking 612% in *gpa1* in the Ws background (Fig. S2D).

### Cantil repression is mediated by a specific Gαβγ complex

Cantil repression by both GPA1 and AGB1 suggested signaling through one, or more, of the 12 heterotrimeric G protein complexes. Given that all three non-dissociable Gβγ dimers cannot form in *agb1*, signaling specificity was investigated in individual null mutants for the three Gγ-subunits (*agg1-1c*, *agg2-1*, *agg3-1* and *agg3-2*) as well as the triple Gγ mutant. Both *agg1* and *agg2* recapitulated the Col-0 cantil frequency phenotype (Fig. S3A-C), while *agg3-1* and *agg3-2* mutants, contrastingly, increased cantil frequency (Figs. S3A,D) and recapitulated the ectopic rippling and stem angle defects of *agb1* (Fig. S3E,F). The $G\gamma_{1/2/3}$ triple mutant likewise morphologically recapitulated *agb1* (Fig. S3G,H), and developed cantils at the same frequency as *agb1-2* and the *gpa1-3 agb1-2* double mutant (Fig. S3I), while *XLG* triple (*xlg1-5 xlg2-1 xlg3-1*) and *RGS1* single (*rgs1-1* and *rgs1-2*) mutants phenocopied Col-0 (Fig. S3J-M). Therefore, cantil repression and maintenance of the stereotypical wild-type inflorescence is mediated specifically by the subunits of a single G protein complex: GPA1-AGB1-AGG3.

### Cantil spurs and stem spikes are repressed by GPA1

Analysis of 1382 cantils revealed GPA1 is uniquely responsible for repressing a distal terminus outgrowth that we call a spur because of its characteristic form (Fig. 2A versus 2B, Fig. S4A) and its diagnostic location: abaxially centered basal to the cantil-pedicel junction. Over 95% of all *gpa1* cantils in the Col-0 background develop spurs (Fig. 2C,D), with 66.6% of all *gpa1* cantils developing solitary spurs, and 28.9% developing spurs that are flanked by reduced, less organized, nub-like growths (Fig. 2C) that are also seen in *agb1* (Figs S1A, S4B). *agb1* mutants do not directly phenocopy *gpa1* spurs, but produce relatively smaller, abaxially off-center, spur-like growths (Fig. S4C) that occur at low frequency (26.2%) (Fig. 2C). Solitary and coincident spur and nub patterning differences between *gpa1* and *agb1* (Fig. 2C) further indicate developmental partitioning between these G protein subunits for these traits. *GPA1* mutants in the Ws background (*gpa1-1, gpa1-2*) (Fig. 2C-E) also produce spurred cantils, which were never observed in wild-type Col-0 or Ws (Fig. 2C,D).

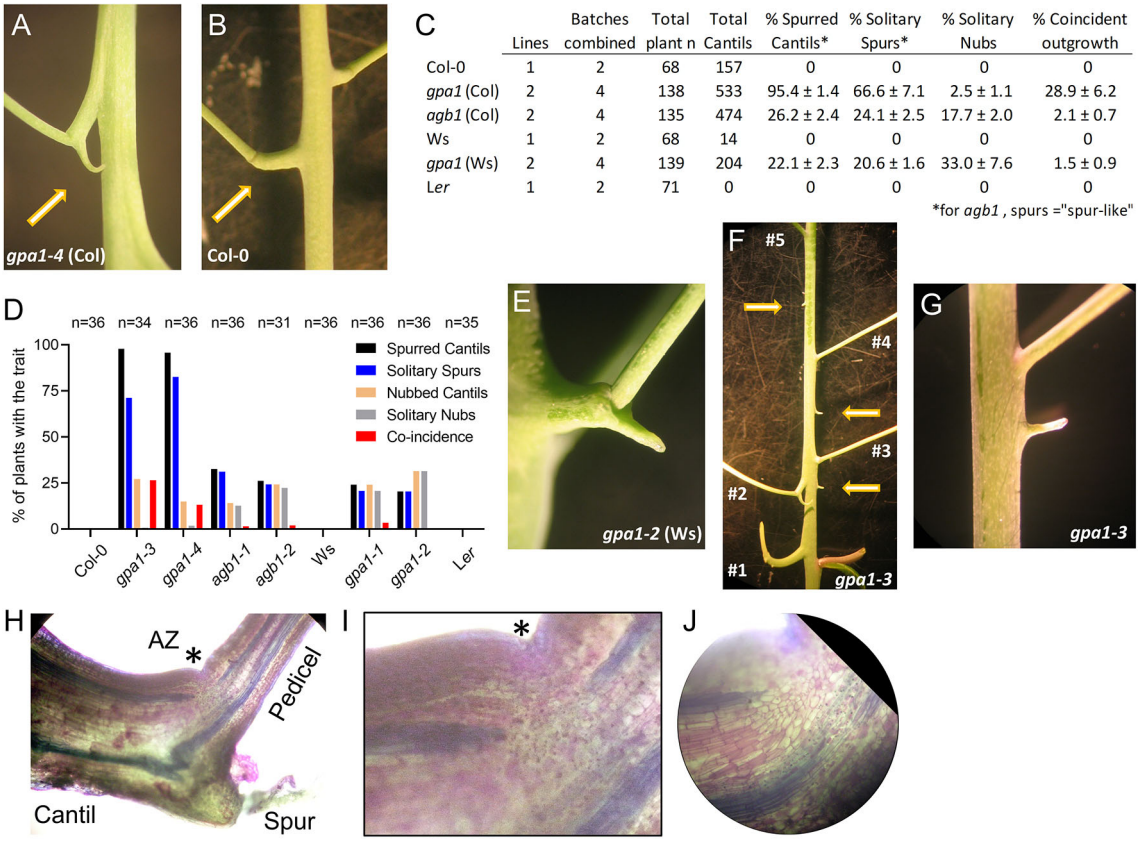


| Lines | Batches combined | Total plant n | Total Cantils | % Spurred Cantils* | % Solitary Spurs* | % Solitary Nubs | % Coincident outgrowth |
|---|---|---|---|---|---|---|---|
| Col-0 | 1 | 2 | 68 | 157 | 0 | 0 | 0 | 0 |
| *gpa1* (Col) | 2 | 4 | 138 | 533 | 95.4 ± 1.4 | 66.6 ± 7.1 | 2.5 ± 1.1 | 28.9 ± 6.2 |
| *agb1* (Col) | 2 | 4 | 135 | 474 | 26.2 ± 2.4 | 24.1 ± 2.5 | 17.7 ± 2.0 | 2.1 ± 0.7 |
| Ws | 1 | 2 | 68 | 14 | 0 | 0 | 0 | 0 |
| *gpa1* (Ws) | 2 | 4 | 139 | 204 | 22.1 ± 2.3 | 20.6 ± 1.6 | 33.0 ± 7.6 | 1.5 ± 0.9 |
| *Ler* | 1 | 2 | 71 | 0 | 0 | 0 | 0 | 0 |

*for *agb1* , spurs ="spur-like"

**Fig. 2. GPA1 represses spur and spike formation.** (A) Short-day *gpa1* cantils produce distal outgrowths designated as spurs (arrow); *gpa1-4* is shown. (B) Wild-type Col-0 cantils do not produce spurs. (C) Quantitative comparison of spur and flanking nub developmental patterns aggregated by genotype, in short days. Solitary spur indicates spur without flanking nubs; solitary nub indicates nub without a spur; coincident outgrowth indicates adjacent spurs and nubs. Percent values are based on the grand mean±s.e.m. of the plant batches for each genotype (i.e. combined chambers and alleles from experiments in Fig. 1J). (D) Representative SD spur and nub patterning for individual alleles expressed as percentage. Data from Chamber #1 experiment are in Fig. 1J. (E) Ws background *gpa1-2* spur. (F) Stem spikes (arrows) occur below spur-less cantils or pedicels. Nodes #1 and #2 are spurred; nodes #3, #4 and #5 are subtended by stem spikes (arrows). (G) Organized growth of an independent spike subtending an archetypal pedicel (*gpa1-3*). (H-J) Internal tissue organization of *gpa1-3* cantils. Vascular tissue is stained with Toluidine Blue. (H) Overview showing that the vestigial abscission zone (AZ, asterisk) develops at the cantil terminus, basal to the pedicel. (I) Magnified view of the AZ (asterisk). (J) Detailed view of an independent *gpa1-3* cantil showing the basal-to-distal transition from rectangular cells to the small AZ cells.

Development (2021) 148, dev195545. doi:10.1242/dev.195545

In theory, the prominent *gpa1* spurs could arise from loss of GPA1 or from enhanced activity of free AGB1-AGG$_{1/2/3}$ dimers; however, double (*gpa1 agb1*) and pentuple (*gpa1 agb1 agg1 agg2 agg3*) knockout lines still produced typical *gpa1* spurs (Fig. S4D-F), demonstrating that GPA1 is the factor repressing spur formation. Shortened *gpa1* cantils frequently show spur formation near the base, and cuffs can form spurs at the stem-cantil junction (Fig. S4G) or fused to the stem (Fig. S4H). When fully displaced, these spurs are abandoned on the stem as independent stem 'spikes' (Fig. 2F,G, Fig. S4H-K). When present, fully formed independent stem spikes always occurred below spur-free *gpa1* cantils, cuffs or archetypal pedicels ($n$=95), but never below spurred cantils ($n$=510) or spurred cuffs ($n$=103), providing further evidence that *gpa1* spurs and spikes share a common origin.

## Cantil development

Cantils form early during inflorescence development, with immature cantils already visible at the onset of M2 elongation (Fig. S4L,M) and well before M3 internode elongation in the flower head. At the M3 node, pedicel elongation occurs prior to cantil elongation, which is followed by spur and stem-spike initiation and elongation (Fig. S4L-N). Cantil and spur tissue is delineated from pedicel tissue by the small cells (Stenvik et al., 2006) that identify a vestigial abscission zone (AZ) (Fig. 2H-J), which is characteristically found at the stem-pedicel boundary in archetypal M3 nodes (Cho and Cosgrove, 2000). Therefore, the AZ functionally demarcates the cantil-pedicel boundary and links the origins of the cantil to the stem proper.

## Cantil natural abundance; global signaling regulation by ERECTA

We screened 10 additional wild-type *Arabidopsis* accessions for SD cantil production and found that cantil competency exhibited natural variant dependency, and ranged from 0.0 to 2.0 cantils/plant (Fig. 3A-E). Notably, MYB13 overexpression in the permissive Dijon-G ecotype produced structures reminiscent of spurred cantils (Kirik et al., 1998). These results indicate cantil formation is widely distributed across *Arabidopsis* accessions, and, as such, identifies a readily available genetic resource to identify additional regulatory factors. To this end, we returned our attention to L*er*.

The widely used L*er* laboratory strain harbors an x-ray induced mutation of *ERECTA* (*ER*) (Torii et al., 1996; Zapata et al., 2016), which encodes a leucine-rich repeat receptor-like kinase (RLK) that directly influences lateral SAM signaling and architecture (Mandel et al., 2014; Zhang et al., 2021). L*er* plants never produced any cantils, cuffs or ectopic rippling while flowering in either SD or LD (Fig. 1M, Fig. S1G,H), and RLKs have recently been implicated as phosphoregulators of plant heterotrimeric G proteins (Chakravorty and Assmann, 2018), suggesting ER may function as a direct positive regulator of cantil formation. Indeed, we found that the Col-0 background *er-105* knockout phenocopies L*er* and fails to produce cantils or cuffs (Fig. 3F), consistent with ERECTA enabling cantil formation in SD.

We genotyped and phenotyped a segregating, all Col-0 background *agb1-2 (–/–) ER/er-105 (+/–)* self-cross population ($n$=47) and found that all of the plants producing cantils and rippled M2-M3 junctions (76.6%, $n$=36) had at least one copy of wild-type *ER* (Fig. 3G). All 11 of the double homozygous *agb1-2 er-105* segregants failed to produce any of the *agb1* traits, demonstrating that *erecta* is functionally epistatic to *agb1* and ERECTA functions as a global regulator of cantil formation.

## Delayed flowering positively regulates cantil and spur development

Cantil expressivity is promoted by short photoperiod, but the underlying signaling response could arise from contemporaneous photoperiod sensing while flowering in SD, or from the temporally delayed transition to flowering that occurs in SD. Neither GPA1 nor

A

| *Arabidopsis* accession | Cantils + Cuffs | Plants | Avg./plant |
|---|---|---|---|
| Dijon-G | 67 | 33 | 2.0 |
| Tsu-1 | 53 | 30 | 1.8 |
| Sei-0 | 20 | 32 | 0.6 |
| Kyoto | 15 | 30 | 0.5 |
| Cvi-1 | 9 | 30 | 0.3 |
| Sp-0 | 6 | 30 | 0.2 |
| W1-0 | 4 | 30 | 0.1 |
| C-24 | 2 | 32 | 0.1 |
| Est-1 | 0 | 30 | 0.0 |
| Bch1-3 | 0 | 30 | 0.0 |

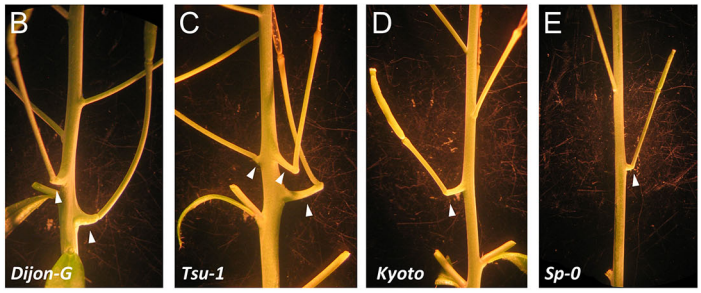


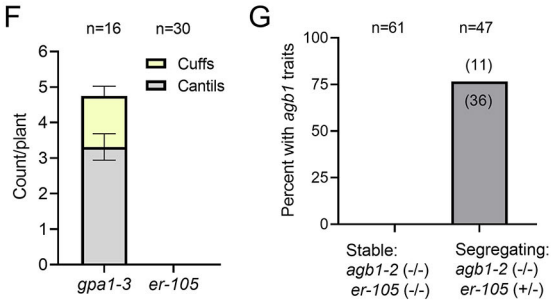





**Fig. 3. Natural abundance of *Arabidopsis* cantils and positive regulation by ERECTA.** (A) Relative abundance of cantils formed by 10 wild-type *Arabidopsis* accessions. (B-E) Representative short-photoperiod cantil formation (arrowheads) in natural accessions: (B) Dijon-G, (C) Tsu-1, (D) Kyoto and (E) Sp-0. (F) Col-0 background *er-105* phenocopies L*er* by failing to develop cantils or cuffs; *gpa1-3* is a positive control (data are mean±s.e.m.). (G) Cantil formation and ectopic rippling is associated with *agb1-2*$^{-/-}$ and the wild-type *ER* allele in a segregating *agb1-2*$^{-/-}$ *er-105*$^{+/-}$ population; plant counts are indicated in parentheses. All 108 stable and segregating plants were genotyped and phenotyped, which certified that only plants homozygous for *er-105*$^{-/-}$ fail to develop *agb1* traits.

Development (2021) 148, dev195545. doi:10.1242/dev.195545

AGB1 influence flowering time in SD (Fig. S5A,B) or LD (Trusov et al., 2008; Urano et al., 2016b); therefore, we assessed null mutants for FLOWERING LOCUS T (FT), a protein that functions as the predominant floral inducer after translocation from rosette leaves to the SAM (Pin and Nilsson, 2012). Col-0 *FT* null plants (*ft-10*) characteristically exhibit delayed flowering in LD (Yoo et al., 2005). We report that *ft-10* plants exhibit delayed flowering in SD (Fig. S5C) and produce cantils in both SD and LD conditions, with equivalent frequency (Fig. 4A).

We used the Col-0 *ft-10* photoperiod-independent cantil competency as a tool to evaluate the observed SD dependence of *gpa1* cantil, spur and spike formation in LDs. Long-day *ft-10* control plants (Fig. 4B,C) produced cantils morphologically identical to Col-0, while, in three experiments, up to 100% of LD *gpa1-3 ft-10* plants produced spurred cantils (Fig. 4D-F). Long-day *gpa1-3 ft-10* also produced stem-spikes in 61.1-68.2% of plants (Fig. 4F,G). Therefore, like cantil formation, spur and spike development is not directly dependent on photoperiod, but on flowering delays. Surprisingly, up to 59.1% of LD *gpa1-3 ft-10* plants also phenocopied the *agb1/agg3* trait of ectopic rippling (Fig. 4D-F), and the rippling frequency followed the spurs/plant and cantils/plant frequencies (Fig. 4F,G). Together, these results provide evidence that the observed photoperiod dependence of natural 'wild-type' cantil formation, and the altered morphology of G-protein mutants, is in fact a function of delayed flowering rather than of day length per se.

## Concluding remarks

Our work directly identifies the existence of a regulatory network (Fig. 4H) that controls organogenesis at the M2-M3 junction and ensures archetypal pedicel emergence directly from M3 nodes. Wild-type *Arabidopsis* accessions are innately capable of producing cantils in SD, and *FT* mutation reveals that delayed flowering is the key expressivity determinant. The entire cantil signaling network is subject to global positive regulation by ERECTA, while negative regulation is provided by the specific GPA1-AGB1-AGG3 heterotrimeric G protein complex subunits, which repress cantil formation and suppress cantil spurs and stem spikes. The loss of GPA1 directly recapitulates the distal protrusions produced by both ROT4 peptide (Ikeuchi et al., 2011) and MYB13 transcription factor (Kirik et al., 1998) overexpression. Furthermore, the loss of AGB1 directly recapitulates the aberrant M2-M3 morphology and altered stem angle produced by TAX1 peptide overexpression (Colling et al., 2015). Potentially, those overexpression phenotypes reflect perturbed G protein signaling through an unknown mechanism.

The stem-like nature and origin of the cantil invites comparison with the pea tendril; the tendril is anatomically similar to the basal rachis (Gould et al., 1994; Tattersall et al., 2005) and exhibits a basal junction lacking axillary meristems (Tattersall et al., 2005), yet is defined as an organ (Hofer and Ellis, 1998; Hofer et al., 2009). Cantil displacement of the vestigial abscission zone from the main stem, coupled with the shared origin of the spur and stem spike, indicate that delayed flowering consequentially induces domains of extended activity in the phase-transitioning SAM. These cantil-related domains provide new targets for understanding and manipulating plant architecture.

In summary, our results lay the foundation for a new area of study, conditional organogenesis at the M2-M3 transition. We identify short photoperiod as the permissive factor, delayed flowering as the

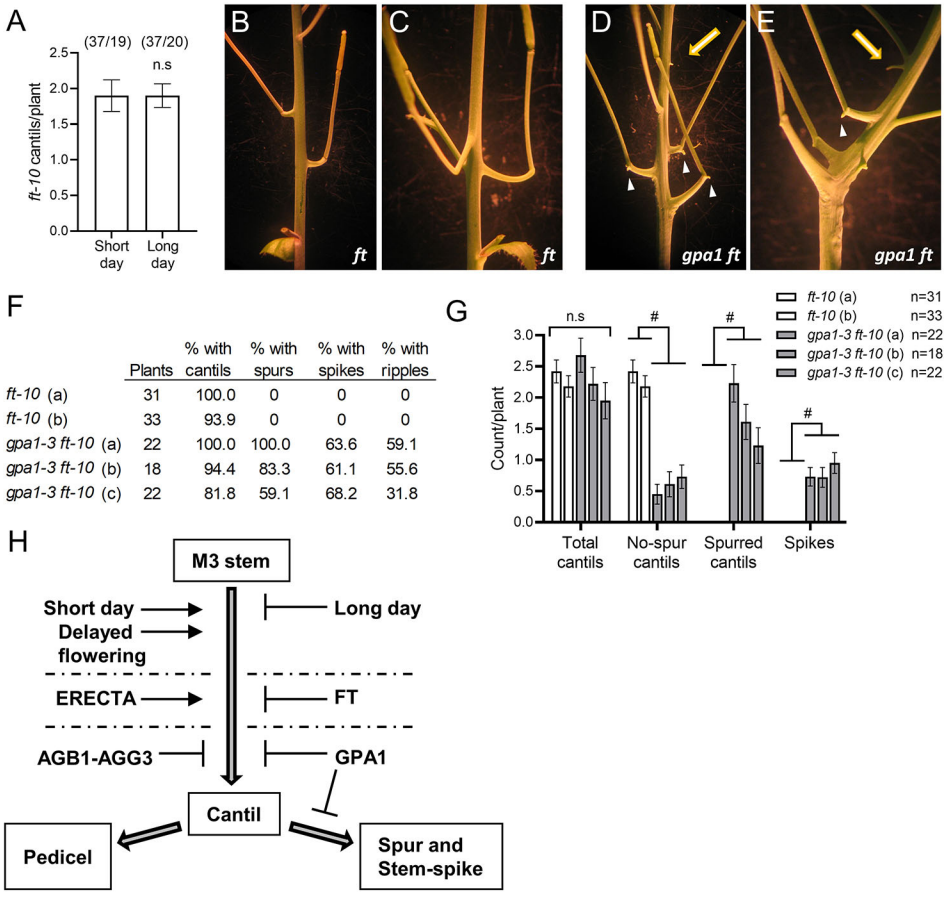


**Fig. 4. Delayed flowering in *ft-10* permits formation of cantils and *gpa1* spurs in long days.** (A) Col-0 background *ft-10* mutants exhibit photoperiod-independent cantil formation; fraction indicates total cantils/total plants. $P$=0.73 (unpaired $t$-test). (B,C) Long-day flowering *ft-10* cantils phenocopy SD flowering Col-0 cantils. (B) Representative LD *ft-10* with spur-less cantils and long internodes. (C) Representative LD *ft-10* with reduced internode length. (D,E) Long-day flowering *gpa1-3 ft-10* phenocopies SD traits of *gpa1* and *agb1*. (D) Long-day *gpa1-3 ft-10* exhibiting *gpa1* traits of spurred-cantils (arrowheads) and a stem spike (arrow). (E) Long-day *gpa1-3 ft-10* exhibiting *gpa1* traits (spurs and spike) as well as the *agb1*/*agg3* traits of strong ectopic rippling and altered stem angle. (F,G) Quantitative comparisons of LD *ft-10* versus *gpa1-3 ft-10* morphology. (F) Trait penetrance, as percentage of plants. Experimental replicates indicated in parentheses. (G) Trait per plant frequencies (data are mean±s.e.m.; significance was tested via one-way ANOVA and Tukey's post-hoc correction). (H) Simplified model of cantil signaling factors.

Development (2021) 148, dev195545. doi:10.1242/dev.195545

cause, and FT, ER and GPA1-AGB1-AGG3 as specific genetic determinants.

## MATERIALS AND METHODS

### Plant materials

*Arabidopsis thaliana* plants were used for all aspects of this study. Columbia (Col-0), Wassilewskija (Ws) and Landsberg erecta (L*er*) are widely available accessions, and were initially obtained from the Arabidopsis Biological Resource Center (ABRC), which was also the source for additional wild-type accessions (Dijon-G, Tsu-1, Sei-0, Kyoto, Cvi-1, Sp-0, W1-0, C-24, Est-1 and Bch1-3).

Columbia (Col-0) background G protein mutants (*gpa1-3, gpa1-4, agb1-1, agb1-2* and *agg3-1*) were individually backcrossed twice to Col-0 and segregated prior to phenotypic quantification. An *agg1-1c agg2-1* mutant originally obtained from the Botella lab (University of Queensland, Brisbane, Australia) was backcrossed to Col-0 to isolate the single *agg* mutants, which were subsequently backcrossed once more to Col-0. Seed bulking was performed before the large-scale experiments, and all of the G-protein mutant parent plants, as well as the wild-type Col-0, Ws and L*er* parent plants were periodically genotyped to verify the absence of other contaminating mutations. The *gpa1-3 agb1-2* double mutant was derived using backcrossed parents. The *gpa1-3 agb1-2 agg1-1c agg2-1 agg3-1* pentuple mutant was generated by crossing *gpa1 agb1* with *agg1-1c agg2-1 agg3-1*. *RGS1* mutants (*rgs1-1, rgs2-1*) were obtained from ABRC, *ft-10* is a GABI-Kat line obtained from NASC and the *er-105* line was a kind gift from the Keiko Torii lab (University of Texas, Austin, USA).

### Plant growth conditions

Seeds were surface sterilized and plated on 0.5× MS medium 0.7% agar plates supplemented with 1% sucrose. After 3 days of stratification at 4° C, the plates were set vertically for germination and exposed to 8 h light/16 h dark at 20°C for 7-10 days, but not longer. Seedlings were transferred to well-watered soil in trays covered by transparent lids, which were adjusted the following day to allow adequate air transfer and moisture release. Vented transparent lids were used to protect the seedlings from growth chamber air flow for ∼2 weeks, and after the seedlings hardened, the lids were removed. Seedlings that failed to thrive were removed. Likewise, weak or otherwise atypical juvenile or mature plants were excluded before the onset of flowering.

Plants were grown in Conviron walk-in chambers with parameters for SD experiments set to 8 h light (140 µmol photons $m^{-2}$ $s^{-1}$) at 21°C, 50% humidity followed by 16 h dark at 19°C, 60% humidity. LD experiments were performed under the same conditions except the light cycle was set to 16 h light/8 h dark. To avoid potential analytical issues caused by comparing data from multiple plantings with differing phenotypic expressivity, we set up a large-scale experiment to simultaneously assess the phenotypes of nine genotypes with 36 seedlings each (324 seedlings in one initial planting). This was replicated in a second large-scale experiment, bringing the total to 648 plants. To validate that our observed phenomena were not unique to a specific growth facility, we performed the two large-scale experiments in two different Conviron walk-in growth chambers. Chamber 1 (Model #MTPS72) has horizontal air handling and precise humidity control, while Chamber 2 (Model #C813) is over twice the size, has air handling via ceiling vents and experiences variable 85-90% humidity in the dark cycle. Additional experiments and validation were performed in Conviron Model #MTPS144 chambers, as well as in similarly set reach-in chambers (pH Environmental Model #CEC38-15-G) with humidity that typically ranged from 35-70% depending on watering status.

To avoid possible nutrient deficiencies arising from nutrient leaching or nutrient depletion during the long growth period, plants were grown in Miracle-Gro potting mix for the large-scale experiments. Soil moisture was regularly checked and the soil was not allowed to fully dry between waterings. As expected for most plant growth traits (e.g. leaf size, plant height and seed yield), cantil expressivity follows plant health and vigor, but fertilized soil is not necessary to observe cantils as they were also observed in plants grown on 1:1 mixes of Miracle-Gro:MetroMix 360, on MetroMix 360 alone and on Sunshine LC1 mix alone. This is exemplified by the comparison of the ∼1.8 cantils/plant formed by *ft-10* grown under SDs and LDs in Miracle-Gro (Fig. 4A), and an additional LD *ft-10* control planted in MetroMix 360, which produced 0.95±0.12 cantils/plant (mean±s.e.m., $n$=36 plants). Growth in miniature pots, or in other conditions that negatively influence plant vigor, can reduce or negate cantil development. As expected for a trait related to flowering, which molecularly initiates prior to visual appearance, inadvertent stress (e.g. drought, flooding or rosette leaf sampling) to juvenile or mature plants can strongly influence cantil frequency, even if the plants appear 'recovered' for several weeks.

### Plant samplings

After full elongation of the primary inflorescence and browning of the first siliques (17-19 weeks after germination for Col-0), the primary inflorescences were removed for inspection under a 1-3.5× dissecting scope. Relevant morphological characteristics were hand-recorded for each assayed plant (short cantils, long cantils, cuffs, spurs, nubs, positions and rippling, etc.) before digital tabulation. At least the first eight or nine pedicels were inspected for each plant, as cuffs were occasionally identified up to nine pedicels away from the M2-M3 junction. Inspection of distal pedicels was also necessary as relatively distal cuffs or very short cantils were observed to occur acropetally to the first 1-2 archetypal pedicels, albeit very rarely. After full inspection of ∼200 long photoperiod grown Col-0 plants, the inspection of LD grown plants was reduced to only the first five pedicels. Likewise, only the first five pedicels were inspected for long photoperiod flowering Ws and L*er*. Representative images were taken through the eyepiece tube of a Bausch & Lomb 0.7-3.0× stereozoom microscope using a Canon G5 camera and a Cole Parmer fiber optic illuminator (Model 41500-50). In many cases, co-florescence below the M2-M3 junction were trimmed for image clarity, leaving a blunt end subtended by a single cauline leaf visible at the bottom of the figure panel: see Fig. 1D,K,L; Fig. 2F; Fig. 3B-E; Fig. 4B-C; Fig. S1C,D; Fig. S3B,C,K,M. For comparison, two visible co-florescences subtended by a single cauline leaf are untrimmed in Fig. 1C but trimmed in Fig. 1D. In Fig. 1E, a trimmed co-florescence is visible but the cauline leaf is out of frame.

### Quantification and statistical analysis

Recorded data were digitized into Microsoft Excel 2016 and imported into GraphPad Prism 8.0 for statistical analysis. As plant sample sizes were unequal in most cases (e.g. large-scale experiments with 31-36 plants per genotype), statistical analysis was performed using one-way ANOVA with a mixed-effects model and Dunnett's correction for multiple comparisons. Multiple comparison tests were restricted to a single wild-type accession control and its associated mutants (e.g. Col-0, *gpa1-3* and *gpa1-4*). Comparison of *ft-10* versus *gpa1-3 ft-10* LD cantil frequency was performed using an all-against-all one-way ANOVA using Tukey's correction for multiple comparisons. Unpaired *t*-tests were employed for two-sample analysis. Graphs were prepared using Prism 8.0.

#### Acknowledgements

We thank Dr Dharmendra Singh, previously from Prof. Timothy McNellis's lab (Pennsylvania State University), members of Prof. Nina Federoff's lab (Pennsylvania State University) and others for early independent confirmation of cantil morphogenesis in their own growth facilities using their own standard protocols. We thank Dr Ángel Ferrero-Serrano for assistance with image collection and Dr David Chakravorty for comments on the manuscript. We thank Profs Keiko Torii (*er-105*) and Phillip Wigge (*ft-10*) for seeds.

#### Competing interests

The authors declare no competing or financial interests.

#### Author contributions

Conceptualization: T.E.G.; Methodology: T.E.G.; Validation: T.E.G.; Formal analysis: T.E.G.; Investigation: T.E.G.; Resources: S.M.A.; Data curation: T.E.G.; Writing - original draft: T.E.G.; Writing - review & editing: S.M.A., T.E.G.; Visualization: T.E.G.; Supervision: S.M.A.; Project administration: S.M.A.; Funding acquisition: S.M.A.

#### Funding

This research was supported by a National Science Foundation grant (MCB-1121612 to S.M.A.), with additional support from a National Science Foundation

grant (MCB-1715826) and by the National Institute of General Medical Sciences of the National Institutes of Health (R01GM126079 to S.M.A.). Deposited in PMC for release after 12 months.

## References

**Anderson, D. J. and Botella, J. R.** (2007). Expression analysis and subcellular localization of the Arabidopsis thaliana G-protein beta-subunit AGB1. *Plant Cell Rep.* **26**, 1469-1480. doi:10.1007/s00299-007-0356-1

**Bommert, P., Je, B. I., Goldshmidt, A. and Jackson, D.** (2013). The maize Galpha gene COMPACT PLANT2 functions in CLAVATA signalling to control shoot meristem size. *Nature* **502**, 555-558. doi:10.1038/nature12583

**Chakravorty, D. and Assmann, S. M.** (2018). G protein subunit phosphorylation as a regulatory mechanism in heterotrimeric G protein signaling in mammals, yeast, and plants. *Biochem. J.* **475**, 3331-3357. doi:10.1042/BCJ20160819

**Chakravorty, D., Gookin, T. E., Milner, M. J., Yu, Y. and Assmann, S. M.** (2015). Extra-large G proteins expand the repertoire of subunits in arabidopsis heterotrimeric G protein signaling. *Plant Physiol.* **169**, 512-529. doi:10.1104/pp.15.00251

**Cho, H.-T. and Cosgrove, D. J.** (2000). Altered expression of expansin modulates leaf growth and pedicel abscission in Arabidopsis thaliana. *Proc. Natl. Acad. Sci. USA* **97**, 9783-9788. doi:10.1073/pnas.160276997

**Colling, J., Tohge, T., De Clercq, R., Brunoud, G., Vernoux, T., Fernie, A. R., Makunga, N. P., Goossens, A. and Pauwels, L.** (2015). Overexpression of the Arabidopsis thaliana signalling peptide TAXIMIN1 affects lateral organ development. *J. Exp. Bot.* **66**, 5337-5349. doi:10.1093/jxb/erv291

**Denay, G., Chahtane, H., Tichtinsky, G. and Parcy, F.** (2017). A flower is born: an update on Arabidopsis floral meristem formation. *Curr. Opin. Plant Biol.* **35**, 15-22. doi:10.1016/j.pbi.2016.09.003

**Dumonceaux, T., Venglat, S. P., Kushalappa, K., Selvaraj, G. and Datla, R.** (2009). Molecular and functional characterization of Brassica BREVIPEDICELLUS orthologs involved in inflorescence architecture. *Botany* **87**, 604-615. doi:10.1139/B09-026

**Giakountis, A., Cremer, F., Sim, S., Reymond, M., Schmitt, J. and Coupland, G.** (2010). Distinct patterns of genetic variation alter flowering responses of arabidopsis accessions to different daylengths. *Plant Physiol.* **152**, 177-191. doi:10.1104/pp.109.140772

**Gookin, T. E. and Assmann, S. M.** (2014). Significant reduction of BiFC non-specific assembly facilitates in planta assessment of heterotrimeric G-protein interactors. *Plant J.* **80**, 553-567. doi:10.1111/tpj.12639

**Gould, K. S., Cutter, E. G. and Young, J. P. W.** (1994). The determination of pea leaves, leaflets, and tendrils. *Am. J. Bot.* **81**, 352-360. doi:10.1002/j.1537-2197.1994.tb15454.x

**Hofer, J. and Ellis, T. H. N.** (1998). The genetic control of patterning in pea leaves. *Trends Plant Sci.* **3**, 439-444. doi:10.1016/S1360-1385(98)01332-6

**Hofer, J., Turner, L., Moreau, C., Ambrose, M., Isaac, P., Butcher, S., Weller, J., Dupin, A., Dalmais, M., Le Signor, C. et al.** (2009). Tendril-less regulates tendril formation in pea leaves. *Plant Cell* **21**, 420-428. doi:10.1105/tpc.108.064071

**Huang, H., Weiss, C. A. and Ma, H.** (1994). Regulated expression of the arabidopsis G protein α subunit gene GPA1. *Int. J. Plant Sci.* **155**, 3-14. doi:10.1086/297142

**Ikeuchi, M., Yamaguchi, T., Kazama, T., Ito, T., Horiguchi, G. and Tsukaya, H.** (2011). ROTUNDIFOLIA4 regulates cell proliferation along the body axis in Arabidopsis shoot. *Plant Cell Physiol.* **52**, 59-69. doi:10.1093/pcp/pcq138

**Ishida, T., Tabata, R., Yamada, M., Aida, M., Mitsumasu, K., Fujiwara, M., Yamaguchi, K., Shigenobu, S., Higuchi, M., Tsuji, H. et al.** (2014). Heterotrimeric G proteins control stem cell proliferation through CLAVATA signaling in Arabidopsis. *EMBO Rep.* **15**, 1202-1209. doi:10.15252/embr.201438660

**Kirik, V., Kölle, K., Wohlfarth, T., Miséra, S. and Bäumlein, H.** (1998). Ectopic expression of a novel MYB gene modifies the architecture of the Arabidopsis inflorescence. *Plant J.* **13**, 729-742. doi:10.1046/j.1365-313X.1998.00072.x

**Mandel, T., Moreau, F., Kutsher, Y., Fletcher, J. C., Carles, C. C. and Eshed Williams, L.** (2014). The ERECTA receptor kinase regulates Arabidopsis shoot apical meristem size, phyllotaxy and floral meristem identity. *Development* **141**, 830-841. doi:10.1242/dev.104687

**Pin, P. A. and Nilsson, O.** (2012). The multifaceted roles of FLOWERING LOCUS T in plant development. *Plant Cell Environ.* **35**, 1742-1755. doi:10.1111/j.1365-3040.2012.02558.x

**Provart, N. J., Alonso, J., Assmann, S. M., Bergmann, D., Brady, S. M., Brkljacic, J., Browse, J., Chapple, C., Colot, V., Cutler, S. et al.** (2016). 50 years of Arabidopsis research: highlights and future directions. *New Phytol.* **209**, 921-944. doi:10.1111/nph.13687

**Stenvik, G. E., Butenko, M. A., Urbanowicz, B. R., Rose, J. K. and Aalen, R. B.** (2006). Overexpression of INFLORESCENCE DEFICIENT IN ABSCISSION activates cell separation in vestigial abscission zones in Arabidopsis. *Plant Cell* **18**, 1467-1476. doi:10.1105/tpc.106.042036

**Tattersall, A. D., Turner, L., Knox, M. R., Ambrose, M. J., Ellis, T. H. N. and Hofer, J. M. I.** (2005). The mutant *crispa* reveals multiple roles for *PHANTASTICA* in pea compound leaf development. *Plant Cell* **17**, 1046. doi:10.1105/tpc.104.029447

**Torii, K. U., Mitsukawa, N., Oosumi, T., Matsuura, Y., Yokoyama, R., Whittier, R. F. and Komeda, Y.** (1996). The Arabidopsis ERECTA gene encodes a putative receptor protein kinase with extracellular leucine-rich repeats. *Plant Cell* **8**, 735-746. doi:10.1105/tpc.8.4.735

**Trusov, Y., Zhang, W., Assmann, S. M. and Botella, J. R.** (2008). Gγ1+Gγ2 not equal to Gβ: heterotrimeric G protein Gγ-deficient mutants do not recapitulate all phenotypes of Gβ-deficient mutants. *Plant Physiol.* **147**, 636-649. doi:10.1104/pp.108.117655

**Urano, D., Chen, J.-G., Botella, J. R. and Jones, A. M.** (2013). Heterotrimeric G protein signalling in the plant kingdom. *Open Biol.* **3**, 120186. doi:10.1098/rsob.120186

**Urano, D., Maruta, N., Trusov, Y., Stoian, R., Wu, Q., Liang, Y., Jaiswal, D. K., Thung, L., Jackson, D., Botella, J. R. et al.** (2016a). Saltational evolution of the heterotrimeric G protein signaling mechanisms in the plant kingdom. *Sci. Signal.* **9**, ra93. doi:10.1126/scisignal.aaf9558

**Urano, D., Miura, K., Wu, Q., Iwasaki, Y., Jackson, D. and Jones, A. M.** (2016b). Plant morphology of heterotrimeric G protein mutants. *Plant Cell Physiol.* **57**, 437-445. doi:10.1093/pcp/pcw002

**Weiss, C. A., Huang, H. and Ma, H.** (1993). Immunolocalization of the G protein alpha subunit encoded by the GPA1 gene in Arabidopsis. *Plant Cell* **5**, 1513-1528. doi:10.1105/tpc.5.11.1513

**Wen, J. and Walker, J.** (2006). CHAPTER 4 - DVL peptides are involved in plant development. In *Handbook of Biologically Active Peptides* (ed. A. J. Kastin), pp. 17-22. Burlington: Academic Press.

**Yoo, S. K., Chung, K. S., Kim, J., Lee, J. H., Hong, S. M., Yoo, S. J., Yoo, S. Y., Lee, J. S. and Ahn, J. H.** (2005). CONSTANS activates SUPPRESSOR OF OVEREXPRESSION OF CONSTANS 1 through FLOWERING LOCUS T to promote flowering in Arabidopsis. *Plant Physiol.* **139**, 770-778. doi:10.1104/pp.105.066928

**Zapata, L., Ding, J., Willing, E. M., Hartwig, B., Bezdan, D., Jiao, W. B., Patel, V., Velikkakam James, G., Koornneef, M., Ossowski, S. et al.** (2016). Chromosome-level assembly of Arabidopsis thaliana Ler reveals the extent of translocation and inversion polymorphisms. *Proc. Natl. Acad. Sci. USA* **113**, E4052-E4060. doi:10.1073/pnas.1607532113

**Zhang, L., Degennaro, D., Lin, G., Chai, J. and Shpak, E. D.** (2021). ERECTA family signaling constrains CLAVATA3 and WUSCHEL to the center of the shoot apical meristem. *Development* **148**, dev189753. doi:10.1242/dev.189753

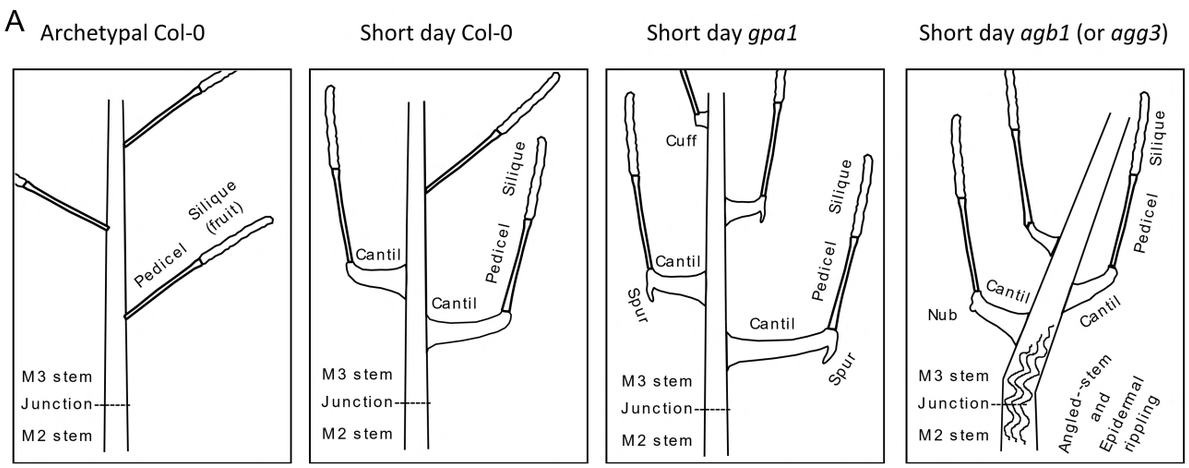


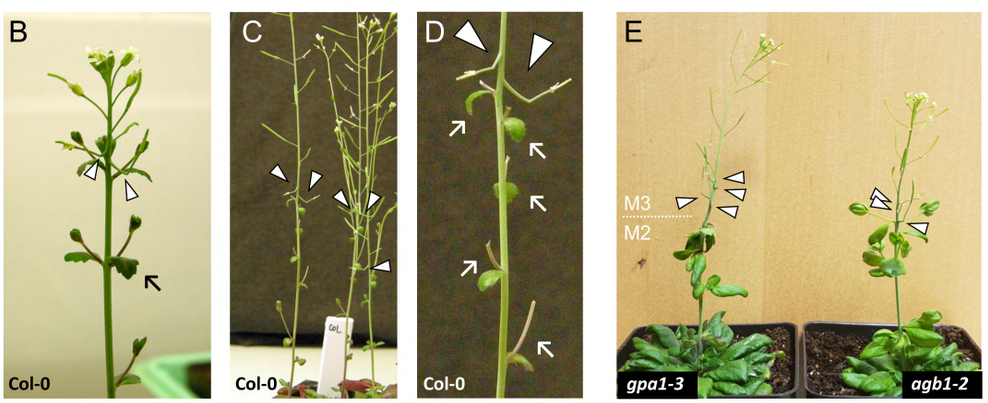



G

| | Daylength | Plants | Cantils |
|---|---|---|---|
| Col-0 | Short | 68 | 157 |
| Ws | Short | 91 | 20 |
| *Ler* | Short | 215 | 0 |
| Col-0 | Long | 727 | 2 |
| Ws | Long | 216 | 0 |
| *Ler* | Long | 252 | 0 |

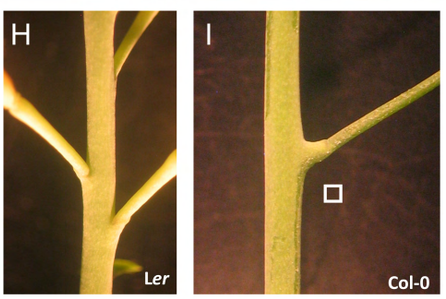


Figure S1

**Figure S1.** Cantil formation

(A) Cartoon overview detailing the morphological features identified in wild-type plants (left two panels), and the unique, additional morphological features (described in Figs. 2-3) found only in the *gpa1*, *agb1* (or *agg3*) G protein mutants (right two panels). B) A mid- development stage Col-0 inflorescence showing two fully formed cantils (arrowheads) distally adjacent to the M2-M3 boundary. A black arrow marks one representative untrimmed co-florescence subtended by a single cauline leaf. C) Fully elongated mature Col-0 inflorescences showing the relative location of cantil development (arrowheads). Note that all three cantil producing Col-0 plants exhibit co-florescences subtended by only a single cauline leaf, as similarly observed for panel S1B. D) Close-up of the left Col-0 plant in panel S1C; the two cantils are marked with arrowheads, five trimmed co-florescences subtended by a single cauline leaf are marked with arrows. E) Whole plant images showing the relative position of cantil development (arrowheads) in *gpa1-3* (left) and *agb1-2* (right). The relative position of the M2-M3 junction is annotated for *gpa1-3.* (F) Cantil formation (*) in the wild-type Ws accession flowering in short days. (G) Count of observed cantils in wild-type accessions flowering in short and long days. The short-day cantil counts were derived from the experiment in Fig. 1J, with the inclusion of additional Ws and L*er* plantings to confirm the low frequency of cantil formation. (H) L*er* fails to form cantils in long or short photoperiods (data in S1G), short-day L*er* shown. Note that the adaxial stem region does not show any signs of bulging or swelling, compare to the Col-0 cuff in Fig. 1E. (I) One of the two total observed cantils (□) formed by Col-0 flowering in long-day (n=727 plants). Both of the observed Col-0 long-day cantils, as well as the three observed long-day Col-0 cuffs described in the main text, developed on pedicel #1 immediately distal to the M2-M3 junction.

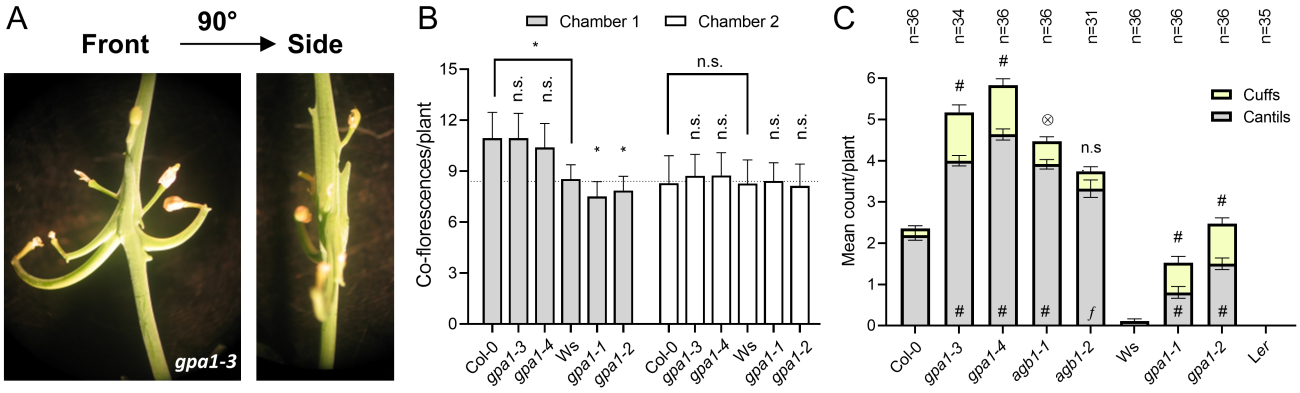


D

| | Daylength | Lines | Total plant n | Total Cantils | Ectopic Rippling | Total % Rippled |
|---|---|---|---|---|---|---|
| Col-0 | Short | wt. | 68 | 157 | 0 | 0 |
| *gpa1* (Col) | Short | 2 | 138 | 533 | 3 | 2.2 |
| *agb1* (Col) | Short | 2 | 135 | 474 | 114 | 84.4 |
| Ws | Short | wt. | 68 | 14 | 0 | 0 |
| *gpa1* (Ws) | Short | 2 | 139 | 204 | 0 | 0 |
| L*er* | Short | wt. | 71 | 0 | 0 | 0 |
| *gpa1-3* (Col) | Long | 1 | 144 | 0 | 0 | 0 |
| *agb1-2* (Col) | Long | 1 | 105 | 0 | 0 | 0 |
| *gpa1-1* (Ws) | Long | 1 | 108 | 0 | 0 | 0 |

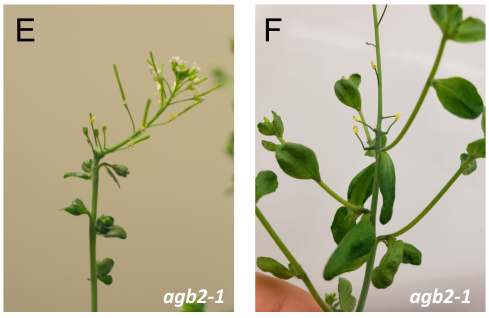


Figure S2

**Figure S2.** G proteins repress cantil morphogenesis.

(A) Extreme planar example of *gpa1* phyllotaxy when flowering in short days; Col-0 background *gpa1-3* shown. (B) Co-florescence frequency analysis of the same plants described in Fig. 1J. Mixed effects analysis (Tukey's multiple comparisons test) shows no significant differences within each genetic background. Within chamber statistical difference from the corresponding wild-type calculated by one-way ANOVA (Dunnett's test), *p<0.05. (C) Quantitative analysis of cuff formation, representative experiment from Chamber 1 from Figure 1J. One-way ANOVA (Dunnett's test, statistical significance for differences in cuff formation from the respective wild type are indicated by symbols above the cuff bars: #p<0.0001, ⊗p=0.0103. Cantil data (and significance symbols within bars) are reproduced from Fig. 1J for ease of reference and to show overall magnitude of the traits. (D) Aggregate count of observed short-day cantils from the experiments in Fig. 1J and lack of cantils in long day. (E) Whole *agb1-2* inflorescence displaying the rippled junction and angled stem phenotypes; the plant is independent of the Fig. 1L example. F) Comparative view of another *agb1-2* inflorescence exhibiting a predominately linear stem at the M2-M3 junction.

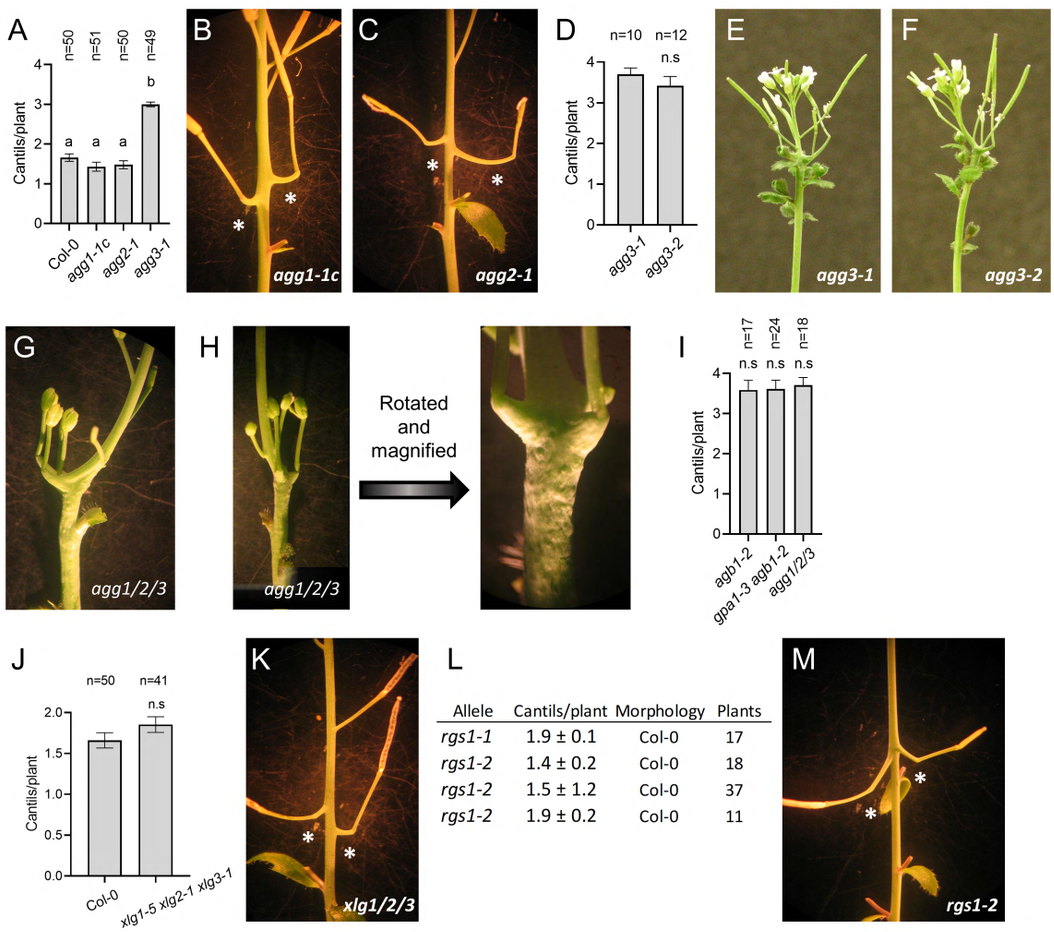


| Allele | Cantils/plant | Morphology | Plants |
|---|---|---|---|
| *rgs1-1* | 1.9 ± 0.1 | Col-0 | 17 |
| *rgs1-2* | 1.4 ± 0.2 | Col-0 | 18 |
| *rgs1-2* | 1.5 ± 1.2 | Col-0 | 37 |
| *rgs1-2* | 1.9 ± 0.2 | Col-0 | 11 |

Figure S3

**Figure S3.** GPA1-AGB1-AGG3: the sole G protein complex subunits modulating cantil development.

Phenotypic display of *AGG*, *XLG*, and *RGS* mutants flowering in short day: (A) *agg3* enhances cantil formation, *agg1* and *agg2* do not increase cantil frequencies over wild-type Col-0, mean±s.e.m. One-way ANOVA (Tukey's test), statistical significance for difference of "b" is $p<0.0001$, while "a" indicates no significant difference among the genotypes. (B) *agg1-1c* and (C) *agg2-1* phenocopy Col-0 and do not display spurs or nubs nor display the *agb1* traits of ectopic rippling and altered stem angle. Asterisks mark the two cantils. (D) *agg3-1* and *agg3-2* exhibit similar cantil frequencies, both of which are increased relative to the Col-0 frequency of ~1.5-2.0 cantils/plant. (E) *agg3-1* and (F) *agg3-2* morphologically phenocopy *agb1*. G) The *agg1-1c agg2-1 agg3-1* triple mutant morphologically phenocopies *agb1.* (H) Another representative *agg1-1c agg2-1 agg3-1* example accompanied by a rotated and magnified image detailing the ectopic rippling caused by *agg3*. (I) *agg1/2/3* phenocopies *agb1* and *gpa1 agb1* cantil frequencies, mean±s.e.m, one-way ANOVA (Tukey's test). (J) The *xlg1-5 xlg2-1 xlg3-1* triple mutant cantil formation frequency is not significantly different from that of Col-0. Unpaired t-test (two-tailed) p-value = 0.154. The *XLG* triple mutant assay shown here and the *AGG* mutant assay in panel "A" were performed side-by-side, therefore panels "A" and "J" share the same Col-0 control, and the results are directly comparable. (K) The *xlg* triple mutant morphologically resembles Col-0, and does not display any of the *gpa1*, *agb1*, or *agg3* traits (i.e. increased cantil frequency, spurs, spikes, nubs, ectopic rippling, or angled stem phenotypes). Asterisks mark the two cantils. (L) Short-day *rgs1-1* and *rgs1-2* mutants develop cantils in the Col-0 frequency range of ~1.5-2.0 cantils/plant (M) *rgs1* phenocopies Col-0 and also fails to develop any *gpa1*, *agb1*, or *agg3* traits; representative *rgs1-2* shown with the two cantils marked with asterisks.

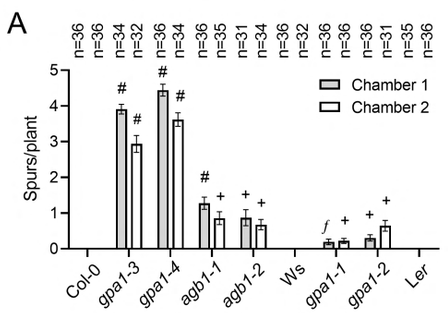



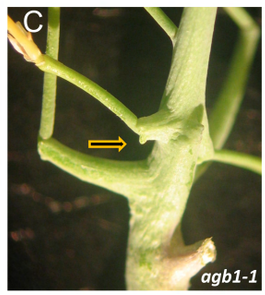


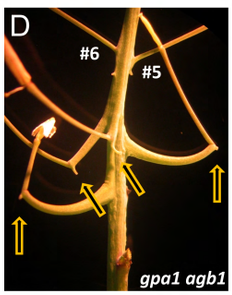


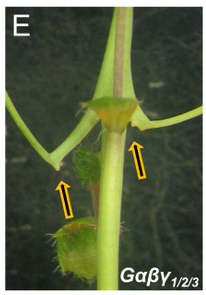


F

| | Batch | Plant n | Plants with spurred cantils | Percent with spurs |
|---|---|---|---|---|
| *gpa1 agb1* | 1 | 15 | 15 | 100.0 |
| *gpa1 agb1* | 2 | 18 | 16 | 88.9 |
| *gpa1 agb1 agg1/2/3* | 1 | 10 | 10 | 100.0 |
| *gpa1 agb1 agg1/2/3* | 2 | 18 | 17 | 94.4 |


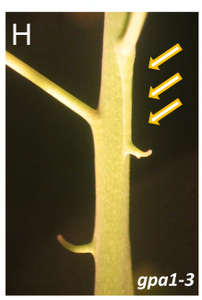



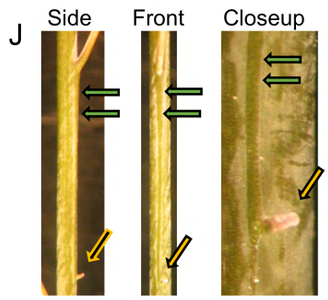


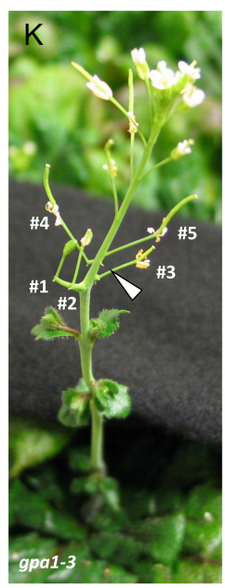



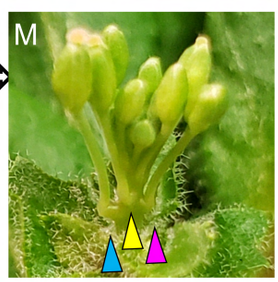


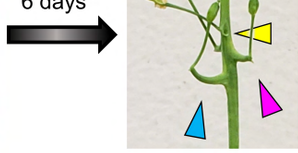


Figure S4

**Figure S4.** Spur and spike repression is a function of GPA1.

(A) Quantification of spur production in the two large-scale experiments detailed in Fig. 1J and 2C. No spurs were observed for Col-0, Ws, or L*er,* and outgrowths in *agb1* are "spur-like", as described in the main text. Mean±s.e.m., one-way ANOVA (Dunnett's test), statistical significance for differences from the respective wild-type are #p<0.0003, +p<0.006, ƒp=0.032. (B) Reduced nub formation in *agb1*; *agb1-2* shown. (C) *agb1* reduced spur-like nub growth with ectopic rippling at the junction; *agb1-1* shown. (D) Representative spurred cantils on *gpa1-3 agb1-2*. Note that the lower pedicel nodes #1-4 have long *gpa1* diagnostic spurs, node #5 has an adnate spur, and the highest node #6 is subtended by an independent spike. (E) Spurred cantil formation in $G\alpha\beta\gamma_{1/2/3}$ (*gpa1-3 agb1-2 agg1-1c agg2-1 agg3-1*). Left side: a long cantil with a classic spur. Right side: a shorter cantil with a spur basally displaced from the cantil terminus. (F) Quantification of *Gαβ* and $G\alpha\beta\gamma_{1/2/3}$ plants; these mutants consistently develop typical *gpa1* spurs. (G) *gpa1* cuff with a spur; *gpa1-2* shown. (H) Adnate spur trailing down the right side of the *gpa1-3* stem. An independent stem spike subtends the pedicel on the left. (I) $G\alpha\beta\gamma_{1/2/3}$ exhibiting an independent stem-spike closely associated with its distal pedicel. White lines in the background are 1 mm ruler markings. (J) A small solitary spike with slightly raised cell files (darker green; "Closeup") tracing back to an archetypal pedicel. Back-tracing cell files are not always raised or always differently colored when present. K) Whole inflorescence image of a *gpa1-3* plant exhibiting four spurred cantils (nodes #1-4) and a distal stem-spike (arrowhead, below pedicel #5). Note that this *gpa1* plant exhibits a minor stem bend, but the junction is not rippled. Image taken at an oblique downward angle to show detail. L) Overview of a *gpa1-3* plant in the early stage of bolting. M) Enlargement showing *gpa1-3* cantil formation preceding M3 internode elongation. Arrowheads mark three spur-less immature cantils. N) After six additional days of growth, four spurred cantils are observed in the mature inflorescence; arrowheads follow the cantils in panel M. The spurs and the distal stem-spike (white arrowhead) were not identifiable in the M3 pre-elongation phase (see panel M).

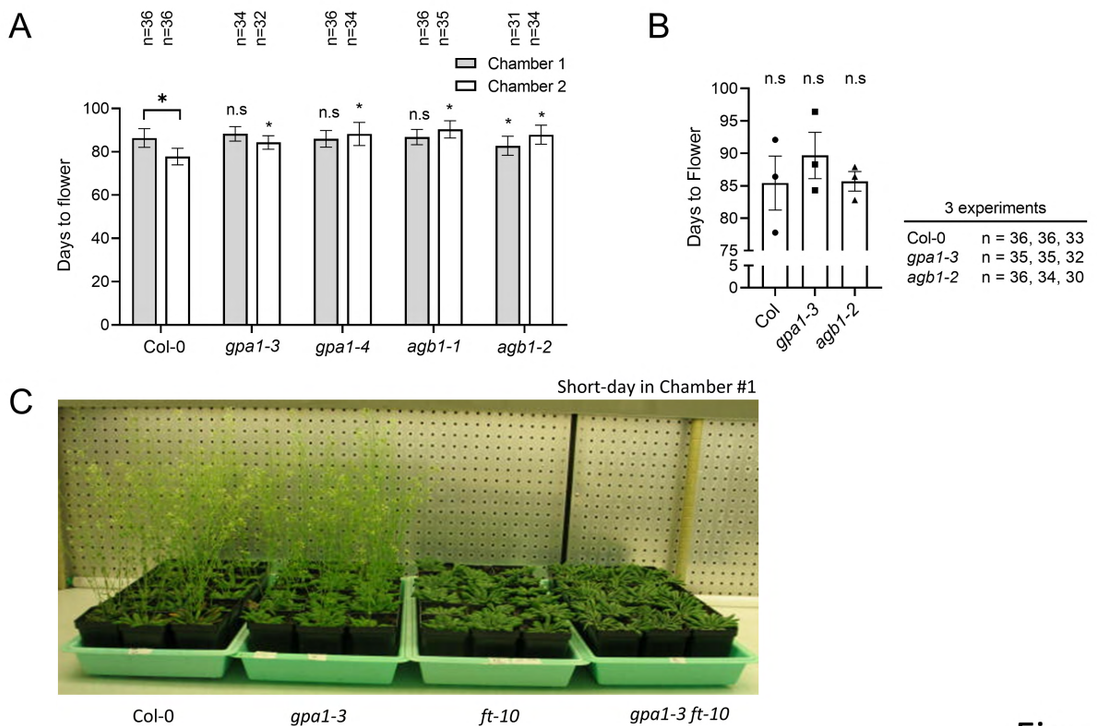


Figure S5

**Figure S5.** Baseline temporal flowering characteristics of Col-0, *gpa1*, *agb1*, and *ft* mutants.

(A) Short-day Col-0 and G protein mutants lack any appreciable difference in flowering time, validating their suitability for comparison. Data were collected from the same plants utilized in our two large-scale experiments described in Fig. 1J, which was performed in two identically programmed, but qualitatively different, short day growth chambers (see Methods in Supplemental Information for chamber details). Plants initiated flowering nearly simultaneously over the course of a week. Col-0 in Chamber 2 flowered several days earlier than those in Chamber 1. Mean±s.e.m., one-way ANOVA (Dunnett's test), statistical significance for differences from the respective wild-type: *p< 0.001. (B). For clarification, we performed a third flowering time experiment: flowering time does not significantly differ between Col-0, *gpa1*, and *agb1* in short-day. One-way ANOVA (Tukey's multiple comparisons test) analysis of all three experiments. Sample sizes from the first two experiments (detailed above in Fig. S2A) are included in the table for clarity and ease of comparison. (C) Co-incident Col-0 and *gpa1-3* (far left and center left) flowering was followed 21 days later by co-incident *ft-10* and *ft-10 gpa1-3* (center right and far right) flowering. At the time the image was captured, 34 of the 36 *ft-10* containing plants had initiated bolting.